GA-A24501

PEDESTAL PROFILES DURING QH–MODE OPERATION ON DIII–D

by
W.P. WEST, C.J. LASNIER, T.A. CASPER,
T.H. OSBORNE, K.H. BURRELL, P.B. SNYDER
D.M. THOMAS, E.J. DOYLE, and A.W. LEONARD

OCTOBER 2003

DISCLAIMER

GA-A24501

PEDESTAL PROFILES DURING QH–MODE OPERATION ON DIII–D

by

W.P. WEST, C.J. LASNIER,[£] T.A. CASPER,[£]
T.H. OSBORNE, K.H. BURRELL, P.B. SNYDER
D.M. THOMAS, E.J. DOYLE,[§] and A.W. LEONARD

This is a preprint of a paper to be presented at the 9th IAEA Tech. Mtg on H-mode Physics and Transport Barriers, San Diego, California, September 24-26, 2003, and to be printed in the *Proceedings*.

[£]Lawrence Livermore National Laboratory, Livermore, CA
[§]University of California, Los Angeles, Los Angeles, CA

Work supported by the U.S. Department of Energy under DE-AC03-99ER54463, W-7405-ENG-48 and DE-FG03-01ER54615.

GENERAL ATOMICS PROJECT 30033
OCTOBER 2003

Pedestal Profiles During QH–mode Operation on DIII–D

W.P. West,[1] C.J. Lasnier,[2] T.A. Casper,[2] T.H. Osborne,[1] K.H. Burrell,[1] P.B. Snyder,[1] D.M. Thomas,[1] E.J. Doyle,[3] A.W. Leonard[1]

[1]General Atomics, P.O. Box 85608, San Diego, CA 92186-5608, USA
[2]Lawrence Livermore National Laboratory, P.O. Box 808, Livermore, CA 94551
[3]University of California, Los Angeles, P.O. Box 951597, Los Angeles, CA 90095-1597

Abstract. The Quiescent High Confinement mode (QH–mode) on DIII–D exhibits an H–mode like edge pedestal, with similar values of pedestal pressure and global energy confinement to ELMing H–mode, but without ELMs. In many cases this mode is observed to reach a nearly stationary operating point, limited in duration only by hardware constraints. This mode is usually obtained in a plasma configuration that is strongly pumped with electron densities at the top of the pedestal below 0.3 of the Greenwald density. Electron temperatures at the top of the pedestal range from 1.2 to 2.2 keV. Ion temperatures at the pedestal are much higher, ranging up to 5 keV. In this paper, we will present edge profiles observed in QH–mode. A selection of these profiles are used as input to the Corsica code to calculate the edge current profile, which is dominated by the bootstrap current. We discuss the implications of these edge profiles on the stability of the QH edge against ballooning/ peeling modes. We also discuss results of experiments in which we attempt to expand the range of edge parameters, especially the edge density, achievable in QH–mode.

1. Introduction

The quiescent high confinement mode [1,2,3] is a stationary mode of tokamak operation discovered on DIII–D that achieves standard H–mode level of confinement with an edge transport barrier, yet does not exhibit the edge relaxation phenomena, ELMs, usually observed in long pulse H–mode operation. QH–mode has been observed in a wide variety of plasma shapes on DIII–D [4], and it has also been observed on other large tokamaks, including Asdex Upgrade [5], JET [6] and JT–60U [7]. Table 1 shows the range of operational parameters in which QH has been observed on DIII–D. There are two significant restrictions to QH operation: (1) it has only been observed in discharges with the direction of neutral heating beam injection opposite to the direction of the plasma current; and (2) typically, QH is observed at low density with the majority of discharges being strongly pumped and having a density below 30% of the Greenwald density limit [8].

This mode of operation is interesting for at least three reasons: (1) the lack of impulsive first wall heating due to the lack of ELMs, (2) the achievement of a stationary state with steep edge pressure gradients and high confinement without ELMs, and (3) compatibility with a core transport barrier without negative impact of ELMs. In this paper, we report on the status of experiments and modeling of the edge stability in QH–mode including the measured edge profiles, comparison of the profiles to those during ELMing phases, and implications with respect to the stability of peeling/ballooning mode.

Table I: Range of parameters for QH–mode on DIII–D

Plasma Parameter	Minimum	Maximum
Average Triangularity	0.15	0.7
Elongation	1.6	2.0
$\bar{n}_e$/Greenwald Limit	0.1	0.5
Line Averaged Density	1.7 x 10^{19} m^{-3}	7.4 x 10^{19} m^{-3}
Plasma Current	–0.68 MA	–2.0 MA
Toroidal Field Magnitude	0.95 T	2.14 T
q_{95}	3.4	5.8

2. Edge Profiles and Stability

The profiles of edge electron density and temperature are measured with the DIII–D Thomson scattering system [9] with very good spatial resolution in the region of the separatrix and H–mode pedestal. The temperature, toroidal and poloidal rotation, and concentration of C^{+6} ions are measured with good spatial resolution using the DIII–D Charge Exchange Recombination (CER) system [10]. Profile measurements during QH operation are shown in Fig. 1 along with fits to the data. Because QH–mode is a quiescent and stationary operating state, data can be taken from an extended period of time for a profile fit. The data shown in Fig. 1 is from a 200 ms window centered at 3000 ms in shot 106919 [3]. The electron density and temperature are fit to a modified tanh function [11] while the ion temperature data are fit to a cubic spline. The mapping of the spatial location of the Thomson and CER channels to the magnetic flux function ψ is done using the equilibrium reconstruction code, EFIT [12]. In Fig. 2, the edge profile fits for the QH phase are compared to an ELMing phase of this discharge at 1200 ms. The data from the ELMing phase are over a 10 ms window, with the specific times for the Thomson scattering data chosen to correspond to times between ELM events. The pressure profiles for the ELMing and QH phases are very similar, but the density is lower in the QH phase and the temperatures are higher. The density behavior reflects the general trend that QH–mode is initiated from an ELMing phase as the density drops due to strong pumping. The total pressure shown in Fig 2 c) is derived from Thomson scattering measurements of n_e and T_e, T_i from CER, the total thermal ion density from the electron density corrected for the dominant impurity density and corrected for the fast ion density as calculated by the transport code ONETWO [13], and the fast ion pressure from ONETWO. The impurity density is obtained from the C^{+6} concentration at the top of the pedestal measured by CER, then assuming that the C^{+6} concentration is constant throughout the pedestal. The stability boundary of coupled peeling/ballooning mode in the edge of a tokamak has recently been explored in theoretical work by Snyder, Wilson, et al. [14]. The stability boundary is shown schematically in Fig. 3.

Ballooning modes are driven unstable as the pressure gradient at the plasma edge increases. Increasing edge current tends to stabilize the ballooning mode, opening up access to the second stable regime. However, a medium n peeling mode is driven unstable as the edge current is increased. Coupled peeling/ballooning modes are driven unstable by a combination of edge current and edge pressure gradient and limit the maximum achievable edge gradients and current. Both rotation and fast ions are known to stabilize MHD activity under some circumstances [15,16]. The effects of toroidal rotation have only recently been added to ELITE, however the analysis presented here does not include either. Since the ELMing and QH phases have very similar pressure gradients, as shown in Fig. 1, it is plausible that a difference in the edge current density is key to the stability.

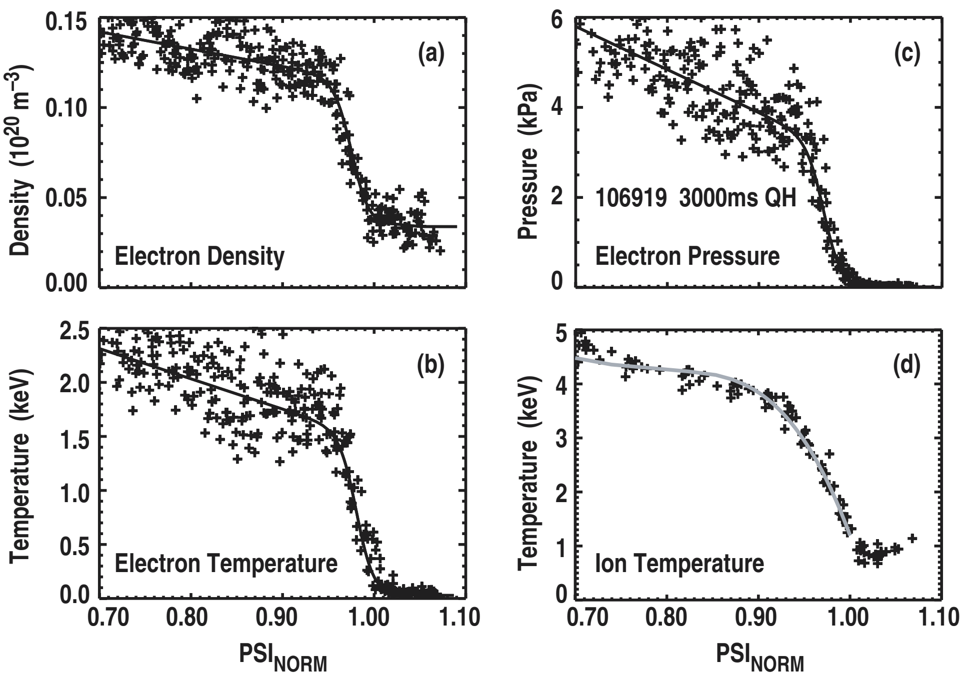

Fig. 1.(a) Edge electron density, (b) temperature, (c) pressure data from Thomson Scatterng with modified tanh fits for a 200 ms window centered at 3000 ms. (d) Edge C^{+6} ion temperature measured with CER along with a cubic spline fit inside the seperatrix.

In discharges with an H–mode-like pedestal, the edge current is comprised primarily of the neoclassical bootstrap current [17,18], J_{BOOT}, driven by the sharp edge gradients in density and temperature.

$$J_{BOOT} = \alpha \frac{\partial n_e}{\partial \rho} + \beta \frac{\partial T_e}{\partial \rho} + \gamma \frac{\partial T_i}{\partial \rho} \quad . \tag{1}$$

The gradients are taken with respect to the toroidal flux coordinate, ρ, and the coefficients α, β, and γ are functions of the plasma shape and collisionality. Typically, $\alpha > \beta > \gamma$, i.e., the density gradient is the strongest driver for the edge current. The edge current density derived by EFIT is not well constrained by the existing set of magnetic diagnostics. A new diagnostic based on Zeeman polarimetry of an injected lithium beam is being developed to provide a good constraint on the edge current in EFIT [19].

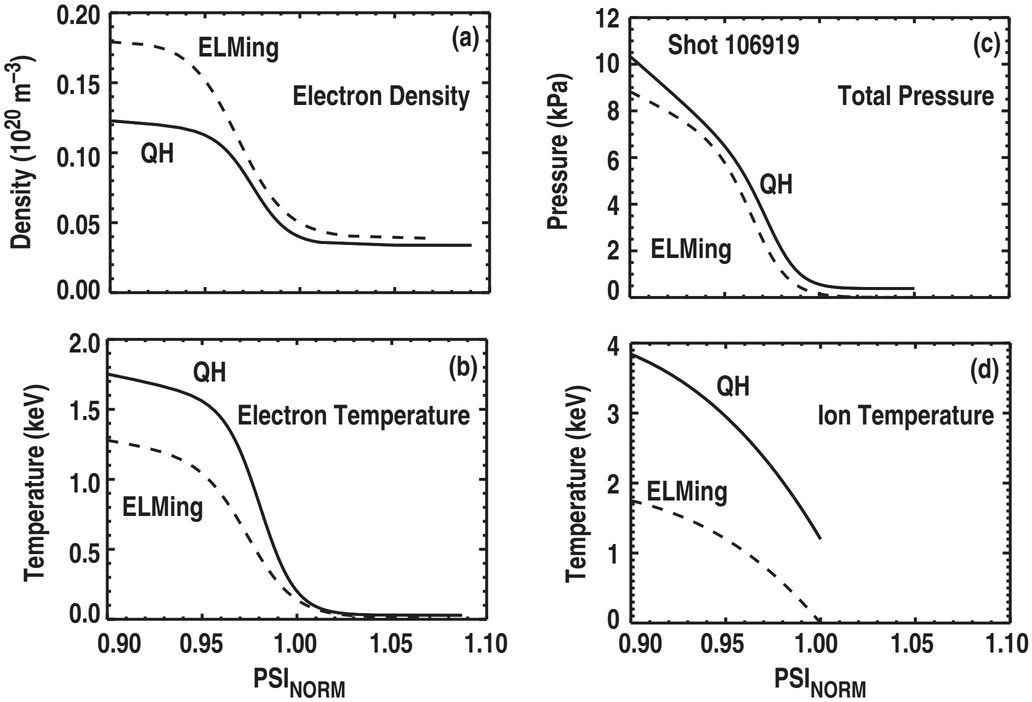

Fig. 2. Modified tanh fits of (a) Edge electron density, (b) temperature, and (c) total pressure and cubic spline fits of (d) the ion temperature for a QH phase (solid), shot 106919 at 3000 ms, and ELMing phase (dashed), shot 106919 at 1210 ms.

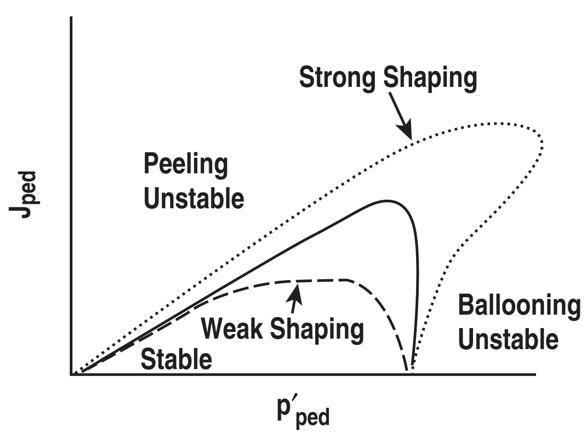

Fig. 3. Schematic of the stability boundary of the coupled peeling/ballooning mode at the plasma edge with respect to the edge pressure gradient and the edge current. The extension of the boundaries to higher gradient and current using strong plasma shaping is shown.

To estimate the edge current, the NCLASS [20] model, embedded in the CORSICA [21] transport code, has been used to calculate the edge bootstrap current from the measured profiles. The gradients of the fitted profiles from Fig. 2, and the calculated edge bootstrap current profiles for the ELMing and QH phases are shown in Fig. 4. While the edge pressure gradient in the QH and ELMing phases are very similar, the calculated edge bootstrap current is significantly higher during the ELMing phase. Qualitatively, these data suggest that the ELMs in this discharge are driven unstable by the higher edge bootstrap current that is driven by the higher edge density gradient.

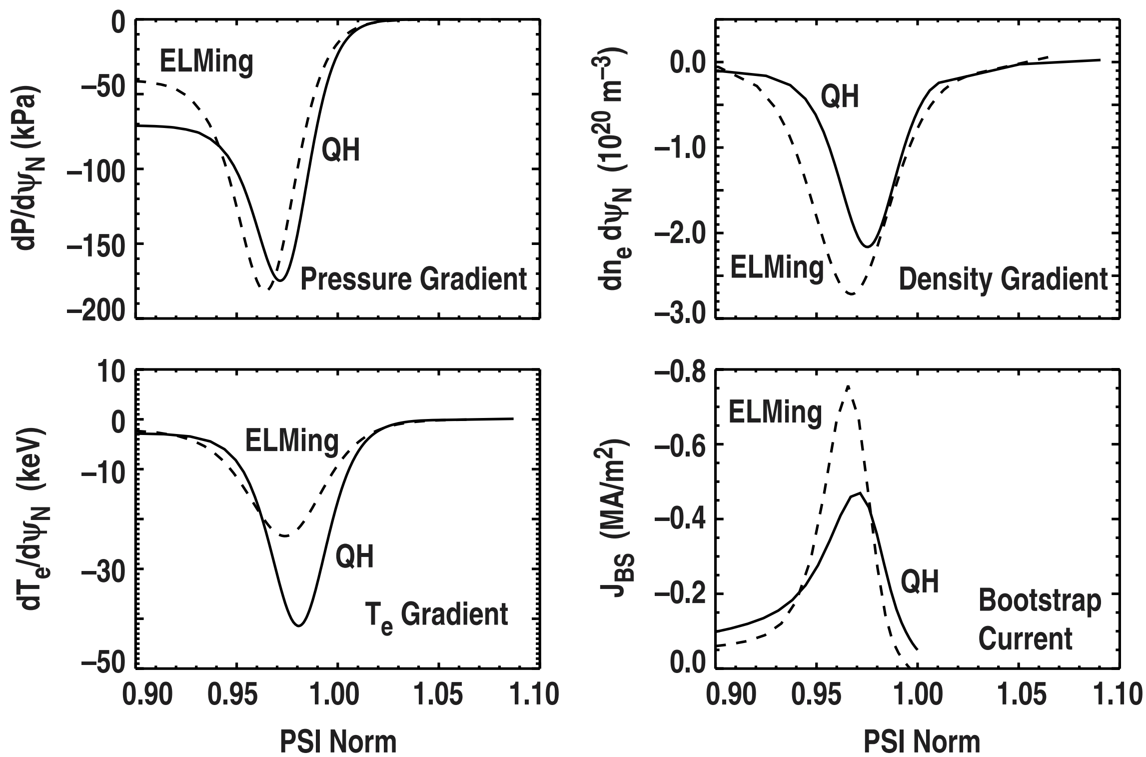

Fig. 4. The edge pressure gradient, density gradient, and calculated edge bootstrap current profiles are shown for the ELMing (dashed) and QH phases (solid) from shot 106919.

3. Current Ramps and Edge Stability

To test the role of the edge current in edge stability, current ramps were performed in the otherwise stationary QH phases of discharges similar to 106919. Since the edge density is low and the edge temperatures are high, the plasma conductivity is high and current penetration times are long. A ramp in the induction rate from the ohmic heating coil will affect the edge current very quickly, but the core current profile will be affected only on the scale of the current penetration time. Figure 5 presents a comparison of two discharges, both with the QH phase initiated in a similar fashion followed by current ramps (1 MA/s) to either increase or decrease the current magnitude. ELMs are seen to return very quickly in the discharge with the increasing edge current, but when the edge current is decreased, the plasma remains in QH–mode. ELMs are also seen to return quickly in a similar discharge with an increasing current ramp rate of only 0.15 MA/s. These data support the hypothesis that the QH–mode is very near a current driven stability limit.

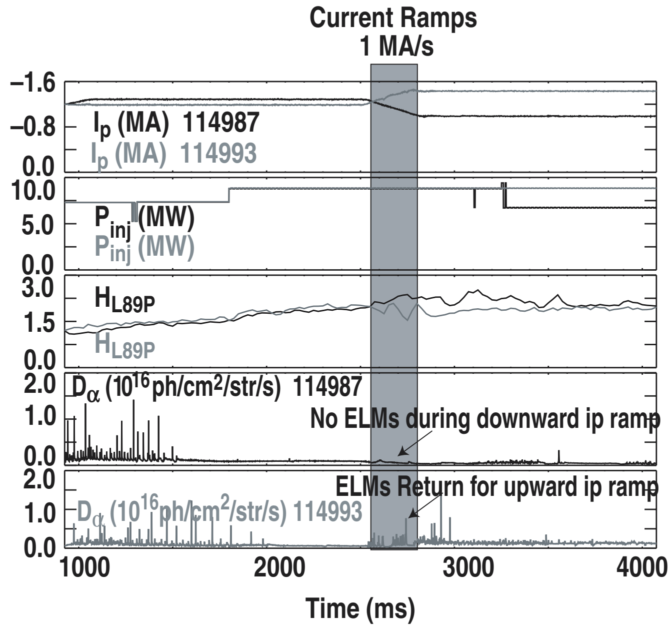

Fig. 5. Time traces of the plasma current, energy confinement H factor (using the ITER89P scaling), and divertor D_α monitors for shots with an increasing and decreasing current ramp are shown.

4. Plasma Shaping and Edge Stability

As seen in Fig. 3, plasma shaping, i.e., elongation and triangularity, tends to push both the current driven and pressure driven stability limits to higher values. Figure 6 shows time traces from discharge 115062 which was scanned to higher elongation and triangularity during QH operation. During this scan, the pedestal density and temperatures increase dramatically, yet the plasma remains in QH–mode. The calculated bootstrap current also rises dramatically due to the shape change, as shown in Fig. 7 for a similar shot, 115099. The observed ability to use shaping to increase both the pedestal pressure and the pedestal current and maintain edge stability is consistent with the peeling/ballooning stability theory (see Fig. 3).

5. Discussion

The kinetic profiles from the experiment are of sufficient resolution and accuracy to provide a quantitative assessment of stability. We are in the process of using the bootstrap current calculated from the measured profiles as a constraint in the equilibrium reconstruction. These equilibria will be tested for stability using ELITE [22], DCON [23], and GATO [24]. In the future, we plan to use the measured magnetic field pitch in the plasma edge from Zeeman polarimetry of a lithium beam as a constraint in the equilibrium reconstruction to determine directly the edge current profile.

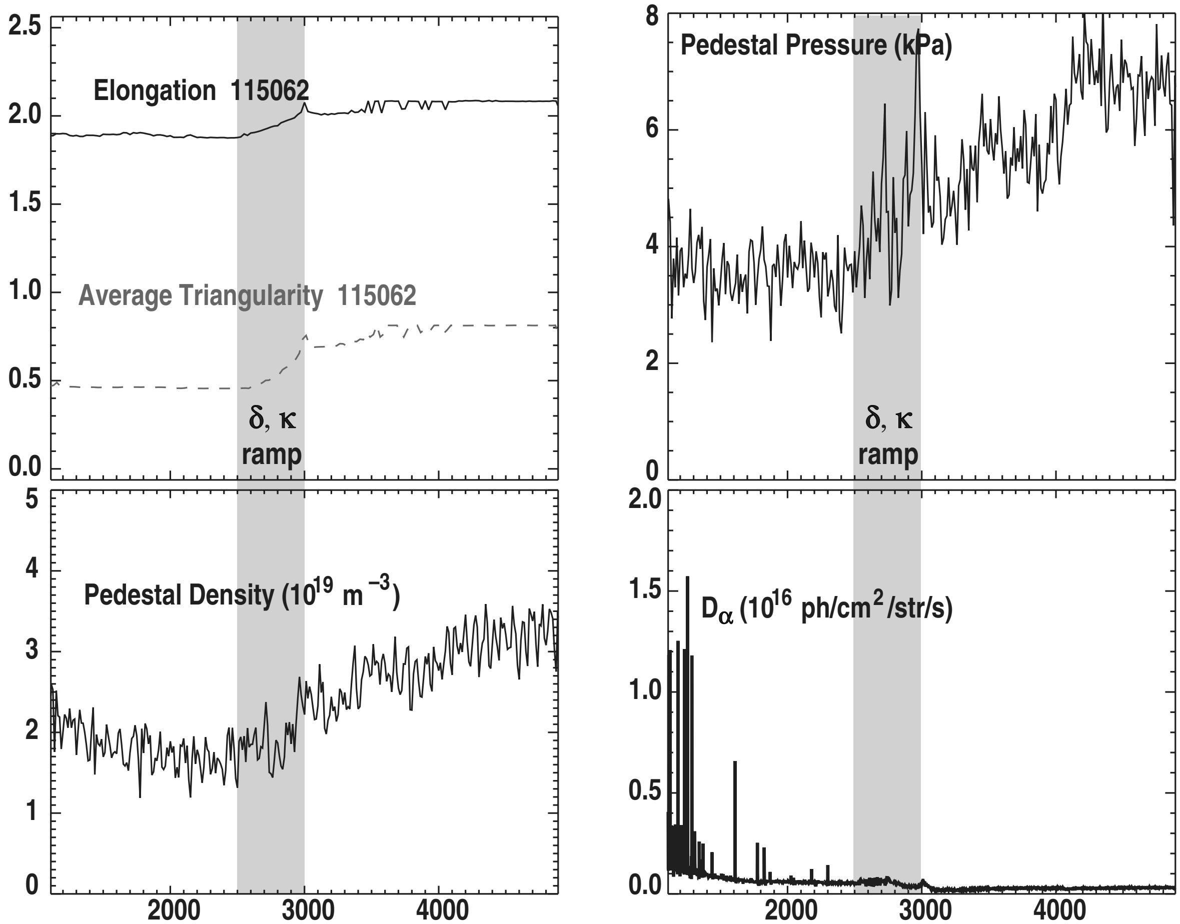

Fig. 6. Time traces of the elongation, triangularity, pedestal density, pedestal pressure, and D_α are shown for a shot with a scan to stronger shape during a QH phase. The plasma current and beam power were 1.4 MA and 8.8 MW.

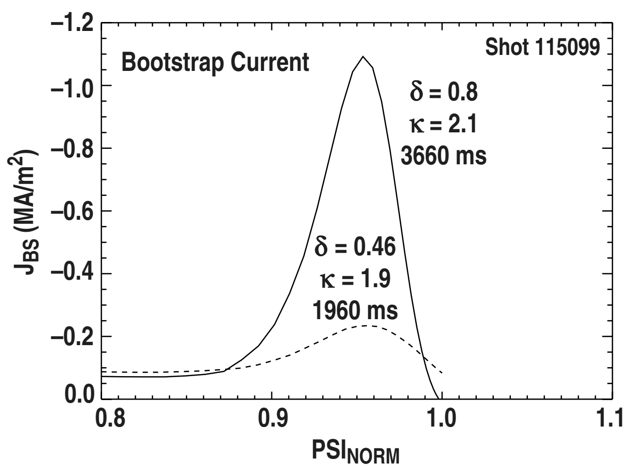

Fig. 7. The calculated edge bootstrap current profiles are shown for shot 115099 during QH phases before (dashed) and after (solid) a sweep to strong shaping similar to shot 115062 in Fig. 6.

6. Conclusions

Qualitative assessment of edge plasma profiles, calculated edge bootstrap current, and current ramps during QH operation suggests that the QH–mode edge plasma is sitting very near the stability limit of a current driven mode, e.g., a coupled peeling/ballooning mode. The specific evidence includes: (1) The preceding ELMing phase and the QH phase of a typical QH discharge have very similar pressure profiles, but the ELMing phase has a higher calculated edge bootstrap current due to a higher edge density gradient; (2) increasing (decreasing) the edge current in QH phase by ramping the ohmic heating coil quickly induces (does not induce) ELMs; and (3) increasing the shaping of a QH discharge allows increased edge current and pressure gradient, in agreement with peeling/ballooning stability theory.

The reasons why the edge current is limited in the QH–mode are not determined, but the low edge density gradients are playing an important role. Low density is achieved in these discharges by strong divertor pumping and high edge particle transport. Low pedestal density can also be achieved in strongly pumped co-injected discharges yet, to date, we have not observed QH–mode in any co-injected discharge. More analysis is required to compare edge currents and stability in QH and similar co-injected discharges. Another unique feature of the QH–mode is a deep narrow radial electric field (E_r) well just inside the separatrix. A thorough discussion of the edge E_r can be found in Burrell, et al., this conference [25].

Acknowledgment

This work supported by the U.S. Department of Energy under Contract Nos. DE-AC03-99ER54463, W-7405-ENG-48 and Grant No. DE-FG03-01ER54615.

References

[1] K.H. Burrell, M.E. Austin, D.P. Brennan, et al., Phys. Plasmas **8** (2001) 2153.

[2] C.M. Greenfield, K.H. Burrell, J.C. DeBoo, et al., Phys. Rev. Lett. **86** (2001) 4544.

[3] W.P. West, M.R. Wade, C.M. Greenfield, et al., Phys Plasmas **9** (2002) 1970.

[4] W.P. West, K.H. Burrell, J. deGrassie, “Quiescent H–mode, an ELM-Free High-Confinement Mode on DIII–D With Potential for Stationary State Operation,” Proc. 30th EPS Conf. on Control. Fusion and Plasma Physics, St. Petersburg, 2003 (European Physical Society, Geneva 2003) CD-ROM.

[5] W. Suttrop. M. Maraschek, G.D. Conway, et al., Plasma Phys. Control. Fusion **45** (2003) 1399.

[6] W. Suttrop, private communication; W. Suttrop, R.A. Pitts, M. Maraschek, et al., “Search in JET for the Quiescent H–mode regime,” Proc. 9th IAEA Tech. Meeting on H–mode Physics and Transport Barriers, San Diego, 2003.

[7] Y. Sakamoto, private communication and Y. Sakamoto, H. Shirai, T. Fujita, et al., Proc. 9th IAEA Tech. Meeting on H–mode Physics and Transport Barriers, San Diego, 2003.

[8] M. Greenwald, J.L. Terry, S.M. Wolfe, S. Ejima, M.G. Bell, S.M. Kaye, G.H. Neilson, Nucl. Fusion **28** (1988) 2199.

[9] T.N. Carlstrom, G.L. Campbell, J.C. DeBoo, Rev. Sci. Instrum. **63** (1992) 4901.

[10] K.H. Burrell, D.H. Kaplan, P. Gohil, et al., Rev. Sci. Instrum. **72** (2001) 1028.

[11] R.J. Groebner, and T.H. Osborne, Phys. Plasmas **5** (1998) 1800.

[12] L.L Lao et al., Nucl. Fusion **30** (1990) 1035.

[13] H.E. St. John, J.R. Ferron, L.L Lao, T.H. Osborn, S.J. Thompson, D. Wroblewski, Plasma Physics and Controlled Nuclear Fusion Research, 1995 (Proc. 15th Int. Conf. Seville, 1994), Vol. **3**, IAEA, Vienna (1995) 603.

[14] P.B. Snyder, H.R. Wilson, J.R. Ferron et al., Phys. Plasmas **9** (2002) 2037.

[15] A.M. Garofalo, T.H. Jensen, L.C. Johnson, R.J. La Haye, et al, Phys. Of Plasmas **9**, 1997 (2002).

[16] W.W. Heidbrink and G.J. Sadler, Nucl. Fusion **34**, 535 (1994).

[17] M.R. Wade, M. Murakami, P.A. Politzer, "Validation of Neoclassical Bootstrap Current Models in the Edge of an H-mode Plasma," submitted to Phys. Rev. Lett. (2003).

[18] D.M. Thomas, A.W. Leonard, L. Lao, et al., "First measurement of pressure gradient driven currents in tokamak edge plasmas", submitted to Phys. Rev. Lett.

[19] D.M. Thomas, Rev. Sci. Instrum. **74** (2003) 1541.

[20] W.A. Houlberg, K.C. Shaing, S.P. Hirshman, and M.C. Zarnsdorf, Phys. Plasma **4** (1997) 3230.

[21] T.A. Casper, et al, Plasma Phys. Control. Fusion **45** (2003) 1193.

[22] H.R. Wilson, P.B. Snyder, et al., Phys. Plasmas **9** (2002) 1277.

[23] A.H. Glasser, LANL Report LA-UR-95-528.

[24] L.C. Bernard, F.J. Helton, R.W. Moore, Comput. Phys. Commun. **24** (1981) 377.

[25] K.H. Burrell, W.P. West, E.J. Doyle, et al., "Edge Radial Electric Field Structure in Quiescent H–mode Plasmas in the DIIII–D Tokamak," Proc. 9th IAEA Tech. Meeting on H–mode Physics and Transport Barriers, San Diego, 2003.